SAR and QSAR in Environmental Research

ISSN: (Print) (Online) Journal homepage: https://www.tandfonline.com/loi/gsar20

Synthesis, biological evaluation and in silico studies of novel thiadiazole-hydrazone derivatives for carbonic anhydrase inhibitory and anticancer activities

H.E. Bostancı, U.A. Çevik, R. Kapavarapu, Y.C. Güldiken, Z.D.Ş. Inan, Ö.Ö. Güler, T.K. Uysal, A. Uytun, F.N. Çetin, Y. Özkay & Z.A. Kaplancıklı

To cite this article: H.E. Bostancı, U.A. Çevik, R. Kapavarapu, Y.C. Güldiken, Z.D.Ş. Inan, Ö.Ö. Güler, T.K. Uysal, A. Uytun, F.N. Çetin, Y. Özkay & Z.A. Kaplancıklı (2023): Synthesis, biological evaluation and in silico studies of novel thiadiazole-hydrazone derivatives for carbonic anhydrase inhibitory and anticancer activities, SAR and QSAR in Environmental Research, DOI: 10.1080/1062936X.2023.2240698

To link to this article: https://doi.org/10.1080/1062936X.2023.2240698

View supplementary material

Published online: 04 Aug 2023.

Submit your article to this journal

View related articles

View Crossmark data

Full Terms & Conditions of access and use can be found at
https://www.tandfonline.com/action/journalInformation?journalCode=gsar20

SAR AND QSAR IN ENVIRONMENTAL RESEARCH
https://doi.org/10.1080/1062936X.2023.2240698

Taylor & Francis
Taylor & Francis Group

Check for updates

Synthesis, biological evaluation and in silico studies of novel thiadiazole-hydrazone derivatives for carbonic anhydrase inhibitory and anticancer activities

H.E. Bostancı[a], U.A. Çevik[b], R. Kapavarapu[c], Y.C. Güldiken[d], Z.D.Ş. Inan[e], Ö.Ö. Güler[f], T.K. Uysal[f], A. Uytun[b], F.N. Çetin[a], Y. Özkay[b] and Z.A. Kaplancıklı[b]

[a]Department of Biochemistry, Faculty of Pharmacy, Cumhuriyet University, Sivas, Turkey; [b]Department of Pharmaceutical Chemistry, Faculty of Pharmacy, Anadolu University, Eskişehir, Turkey; [c]Department of Pharmaceutical Chemistry and Phytochemistry, Nirmala College of Pharmacy, Atmakur, India; [d]Department of Neurology, Kocaeli University Research and Application Hospital, İzmit, Turkey; [e]Department of Histology and Embryology, Sivas Cumhuriyet University, Sivas, Turkey; [f]Department of Medical Biology, Faculty of Medicine, Ankara Yildirim Beyazit University, Ankara, Turkey

ABSTRACT

Thiadiazole and hydrazone derivatives (5a–5i) were synthesized and their chemical structures were verified and described by ^{1}H NMR, ^{13}C NMR, and HRMS spectra. Three cancer cell lines (MCF-7, MDA, and HT-29) and one healthy cell line (L929) were used to test the cytotoxicity activity of synthesized compounds as well as their inhibitory activity against carbonic anhydrase I, II and IX isoenzymes. Compound 5d (29.74 µM) had a high inhibitory effect on hCA I and compound 5b (23.18 µM) had a high inhibitory effect on hCA II. Furthermore, compound 5i was found to be the most potent against CA IX. Compounds 5a-5i, 5b and 5i showed the highest anticancer effect against MCF-7 cell line with an IC_{50} value of 9.19 and 23.50 µM, and compound 5d showed the highest anticancer effect against MDA cell line with an IC_{50} value of 10.43 µM. The presence of fluoro substituent in the *o*-position of the phenyl ring increases the effect on hCA II, while the methoxy group in the *o*-position of the phenyl ring increases the activity on hCA I as well as increase the anticancer activity. Cell death induction was evaluated by Annexin V assay and it was determined that these compounds cause cell death by apoptosis. Molecular docking was performed for compounds 5b and 5d to understand their biological interactions. The physical and ADME properties of compounds 5b and 5d were evaluated using SwissADME.

ARTICLE HISTORY
Received 1 April 2023
Accepted 5 July 2023

KEYWORDS
Thiadiazole; hydrazone; carbonic anhydrase; anticancer; molecular docking

Introduction

Carbonic anhydrases (CAs), which have Zn^{2+} ions in their active site, convert carbon dioxide (CO_2) and water into proton and bicarbonate anion (HCO_3^-) [1–4]. There are 15 different CA isoforms in humans, each of which has unique molecular characteristics,

CONTACT H.E. Bostancı erenbostanci@cumhuriyet.edu.tr
Supplemental data for this article can be accessed at: https://doi.org/10.1080/1062936X.2023.2240698
© 2023 Informa UK Limited, trading as Taylor & Francis Group

subcellular localizations, and tissue distribution [5,6]. These isoforms can be categorized according to where they are found;

(a) cytosolic isoforms: CA I, CA II, CA III, CAVII, CAXIII
(b) transmembrane bound isoforms: CA IV, CA IX, CA XII, CA XIV
(c) mitochondrial isoforms: CA VA, CAVB
(d) CA VI, which found in body fluids like saliva [7–10].

Numerous physiological and cellular processes, such as the transport of carbon dioxide, the regulation of acid-base balance, the secretion of electrolytes, and biosynthetic pathways all depend on these enzymes [5,11]. The bioactivities of hCA activators and/or inhibitors include effects that are diuretic, anti-Alzheimer, anti-obesity, anti-epileptic, anti-cancer, and anti-infective [12–14]. The isoenzymes in this class that are expressed in erythrocytes are therefore hCA I (expressed in erythrocytes) and hCA II (expressed in bone osteoclasts, gastrointestinal tract, testis, brain, erythrocytes, kidney, gastrointestinal tract, lung and eye) [15].

The sulphonamide family and their derivatives are the classical carbonic anhydrase inhibitors (CAIs). Due to off-target inhibition, the available CAIs function systemically and bind non-specifically, producing a variety of undesirable side effects. Therefore, the requirement for selecting non-classical CAIs is critical [16].

Cancer is a disease that affects people in many different ways. These impacts range from its detrimental impact on a patient's physical and emotional health, as well as their ability to work and live a full life, to its financial impact due to the high costs and drawn-out nature of cancer treatment. Scientists' efforts to find novel, efficient medications have accelerated in light of the disease seriousness and severe effects on human life. Anticancer medications have recently focused on the human carbonic anhydrase (hCA) enzymes [17].

Depending on the condition of the tumour cells, various pathways contribute to the development of cancer in tissues. In hypoxic conditions, cancer cells activate different metabolic pathways leading to the production of acidic metabolites. An obvious selective benefit for the growth of tumour masses is provided by the extracellular environment's increased acidity. Intracellular and extracellular acidosis threatens cell viability, and low pH levels can disrupt various biological activities. However, tumour cells can adapt to pH changes. One of these factors, carbonic anhydrase (CA) IX, is overexpressed in hypoxia. The increased overexpression of the CA IX isoenzyme in this area and the reliance of pH control on this enzyme explain the necrosis around the tumour [18–20]. Furthermore, among the CA isoforms, CA II is commonly related with a variety of cancers. A recent study found that CA II is expressed in the endothelium of neovessels in melanoma, oesophageal, renal, and lung malignancies. In other research, CA II is linked to the critical target antigen that stimulates an autoantibody response in melanoma patients [21]. Additionally, some recent studies revealed the overexpression of CA II in a variety of cancer types [22,23].

Five-membered heterocycle-containing molecules have drawn more and more attention in recent years when it comes to creating anticancer drugs. The 1,3,4-thiadiazole system is regarded as one of the promising structures. There are numerous studies on the 1,3,4-thiadiazole derivatives' ability to treat tumours [24,25]. Different medicinal medications available on the market contain thiadiazole derivatives (Figure 1). For instance,

acetazolamide and methazolamide are powerful carbonic anhydrase inhibitors. Megazol is an antitrypanosomal drug, sulfamethizole has antibacterial activity. Members of the first generation of the cephalosporin family include cefazolin and cefazedone [26].

Due to their intriguing features, *N*-Acylhydrazones with the -CO-NH-N= unit have attracted attention for a long time and have been used in medicine [27]. The increased activity of acyl hydrazone fragments attached to heterocyclic systems was demonstrated. The potential of acyl hydrazones to create a hydrogen bond with the molecular target is what accounts for their bioactivity. Additionally, because to the blocking effects of NH_2 groups, investigations in the literature have indicated that acyl hydrazones are less hazardous than hydrazides. The significance of manufacturing chemicals generated from acyl hydrazone was further reinforced by these research findings [28].

The facts cited above inspired us to create hybrid molecules that combine the two crucial moieties, hydrazone and thiadiazole, into a single molecule. In order to create novel medication candidates with less cytotoxic effects, this was done. The synthetic substances were tested against hCA I, II and IX, a cancer cell line, and a healthy cell line. Several spectral methods, such as ^{1}H NMR, ^{13}C NMR, and HRMS, were used to clarify the structures of the compounds. Thereafter, the molecular docking of the active compounds at hCA I and hCA II active sites was performed and the obtained results revealed that these compounds interacted with the important amino acids of the active site. In addition, the ability of active compounds to induce apoptosis was also investigated by the Annexin V binding assay.

Several kinds of proteins have different influence on how the cell cycle behaves. Cells stop their cell cycle in the G1/S, S, or G2/M phase and activate checkpoint mechanisms that control replication and DNA repair when DNA damage occurs.

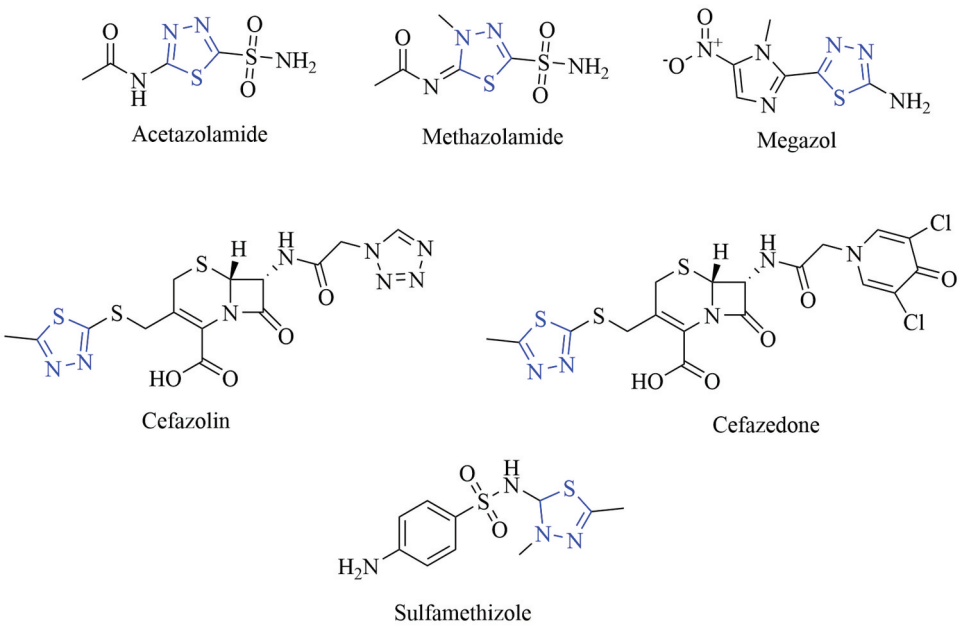

Figure 1. Representative thiadiazole-based drug molecules.

The G1 checkpoint and the G2 checkpoint are often linked to the DNA damage checkpoint pathway, and p21, which is controlled by p53, is crucial to the G1 checkpoint. p21 suppresses the effect of DNA replication through a complex process.

One of the transcriptional targets of the tumour suppressor p53 protein, p21, inhibits the activity of checkpoints in the early stage of mitosis and subsequently arrests the cell cycle. Cell cycle checkpoints (G1, S, and G2/M) are triggered and cell cycle progression renders cell death unavoidable when DNA damage is generated in a cell [29].

In order to understand the anticancer effect of thiadiazole and hydrazone derivatives on HT-29, MCF-7, and MDA cells, it is important to determine the intracellular localization of the p21 protein, which causes cancer cells to stop the cell cycle and go to apoptosis. The anticancer activity of the compound 5f component in the HT29 cell line, the compound 5b component in the MCF7 cell line, and the compound 5d component in the MDA cell line were also supported by the high localization of the p21 antibody.

Materials and methods

Chemistry

General procedure for the synthesis of N-*(4-chlorophenyl)hydrazinecarbothioamide (1)*

A derivative of 4-chloroisothiocyanate (0.02 mol) was dissolved in ethanol and put in an ice bath. The reaction content received dropwise additions of hydrazine hydrate (0.024 mol) in ethanol. The precipitated product was filtered off following the completion of the dripping procedure.

General procedure for the synthesis of 5-(4-chlorophenylamino)-1,3,4-thiadiazole-thiol (2)

N-(4-chlorophenyl)hydrazinecarbothioamide (1) was dissolved in ethanol, and the reaction mixture also contained carbon disulphide and sodium hydroxide. For 3–4 hours, the reaction was stirred while in reflux. The reaction's product was then precipitated with HCl acid after being put into freezing water at the conclusion of the process.

General procedure for the synthesis of 2-((5-((4-chlorophenyl)amino)-1,3,4-thiadiazol-2-yl)thio)acetate (3)

Chloroethylacetate and 5-(4-chlorophenylamino)-1,3,4-thiadiazole-thiol (2) were dissolved in acetone. To the mixture was added potassium carbonate. For two hours at 40°C, the mixture was stirred in a reflux pan. Filtered out, rinsed with water, and crystallized from ethanol was the precipitated product.

General procedure for the synthesis of 2-((5-((4-chlorophenyl)amino)-1,3,4-thiadiazol-2-yl)thio)acetohydrazide (4)

Hydrazine hydrate was added after the 2-((5-((4-chlorophenyl)amino)-1,3,4-thiadiazol-2-yl)thio)acetate (3) was dissolved in ethanol. The mixture was heated for two hours at reflux, and the precipitated portion was removed by filtering.

General procedure for the synthesis of 2-((5-((4-chlorophenyl)amino)-1,3,4-thiadiazol-2-yl)thio)-N′-(substituted benzylidene) acetohydrazide (5a–5i)

A small amount of ethanol was used to dissolve 2-((5-((4-chlorophenyl)amino)-1,3,4-thiadiazol-2-yl)thio)acetohydrazide (4), and then acetic acid and an aldehyde derivative (0.001 mol) were added. Two hours of reflux heating the mixture resulted in the precipitate, which was filtered out and crystallized from butanol.

N′-(benzylidene)-2-((5-((4-chlorophenyl)amino)-1,3,4-thiadiazol-2-yl)thio) acetohydrazide (5a)

Yield: 77%, M.P. = 216°C. ^{1}H-NMR (300 MHz, DMSO-d_6): δ: 4.46 (2H, s, -S-CH_2), 7.35–7.38 (2H, m, -Aromatic CH), 7.40–7.44 (3H, m, Aromatic CH), 7.57–7.61 (2H, m, Aromatic C-H), 7.66–7.69 (2H, m, Aromatic C-H), 8.02 (1H, s, -CH), 10.48 (1H, s, NH), 11.67 (1H, s, NH). ^{13}C-NMR (75 MHz, DMSO-d_6): δ: 36.31, 119.38, 125.84, 127.36, 129.26, 130.43, 134.38, 139.71, 144.29, 147.71, 153.53, 165.09, 169.13. HRMS (m/z): $[M+H]^+$ calcd for $C_{17}H_{14}N_5OS_2Cl$: 404.0401; found: 404.0407.

2-((5-((4-chlorophenyl)amino)-1,3,4-thiadiazol-2-yl)thio)-N′-(2-fluorobenzylidene) acetohydrazide (5b)

Yield: 75%, M.P. = 188°C. ^{1}H-NMR (300 MHz, DMSO-d_6): δ: 4.45 (2H, s, -S-CH_2), 7.23–7.28 (2H, m, -Aromatic CH), 7.35–7.38 (2H, m, Aromatic CH), 7.42–7.47 (1H, m, Aromatic CH), 7.57–7.60 (2H, m, Aromatic C-H), 7.85–7.91 (1H, m, Aromatic C-H), 8.22 (1H, s, -CH), 10.48 (1H, s, NH), 11.77 (1H, s, NH).^{13}C-NMR (75 MHz, DMSO-d_6): δ: 36.22,116.42 (d, J = 20.58 Hz), 119.38, 125.37, 125.85, 126.81 (d, J = 2.5 Hz), 129.35, 132.34 (d, J = 8.42 Hz), 132.61 (d, J = 8.43 Hz), 137.10, 139.69, 140.48 (d, J = 4.61 Hz),159.47, 163.97 (d, J = 177.48 Hz), 169.26. HRMS (m/z): $[M+H]^+$ calcd for $C_{17}H_{13}N_5OFS_2Cl$: 422.0307; found: 422.0327.

2-((5-((4-chlorophenyl)amino)-1,3,4-thiadiazol-2-yl)thio)-N′-(2-chlorobenzylidene) acetohydrazide (5c)

Yield: 82%, M.P. = 198°C. ^{1}H-NMR (300 MHz, DMSO-d_6): δ: 4.46 (2H, s, -S-CH_2), 7.34–7.39 (2H, m, -Aromatic CH), 7.39–7.44 (2H, m, Aromatic CH), 7.47–7.53 (1H, m, Aromatic CH), 7.57–7.62 (2H, m, Aromatic C-H), 7.93–7.97 (1H, m, Aromatic C-H), 8.40 (1H, s, -CH), 10.47 (1H, s, NH), 11.84 (1H, s, NH). ^{13}C-NMR (75 MHz, DMSO-d_6): δ: 36.26, 119.38, 125.86, 127.31, 128.02, 129.34, 130.32, 131.81, 133.46, 139.69, 140.31, 143.61, 164.08, 165.21, 169.32. HRMS (m/z): $[M+H]^+$ calcd for $C_{17}H_{13}N_5OS_2Cl_2$: 438.0011; found: 438.0029.

2-((5-((4-chlorophenyl)amino)-1,3,4-thiadiazol-2-yl)thio)-N′-(2-methoxybenzylidene) acetohydrazide (5d)

Yield: 71%, M.P. = 203°C. ^{1}H-NMR (300 MHz, DMSO-d_6): δ: 3.84 (3H, s, -OCH_3), 4.44 (2H, s, -S-CH_2), 6.96–7.01 (1H, m, -Aromatic CH), 7.05–7.08 (1H, m, Aromatic CH), 7.35–7.41 (3H, m,

Aromatic CH), 7.57–7.62 (2H, m, Aromatic C-H), 7.78–7.81 (1H, m, Aromatic C-H), 8.35 (1H, s, -CH), 10.47 (1H, s, NH), 11.62 (1H, s, NH). ^{13}C-NMR (75 MHz, DMSO-d_6): δ: 36.37, 56.12, 112.25, 119.38, 121.22, 122.40, 125.88, 129.35, 131.92, 139.71, 139.94, 143.20, 158.11, 163.67, 165.10, 168.99. HRMS (m/z): $[M+H]^+$ calcd for $C_{18}H_{16}N_5O_2S_2Cl$: 434.0507; found: 434.0506.

2-((5-((4-chlorophenyl)amino)-1,3,4-thiadiazol-2-yl)thio)-N′-(4-fluorobenzylidene) acetohydrazide (5e)

Yield: 87.5%, M.P. = 221°C. ^{1}H-NMR (300 MHz, DMSO-d_6): δ: 4.44 (2H, s, -S-CH_2), 7.22–7.28 (2H, m, -Aromatic CH), 7.35–7.39 (2H, m, Aromatic CH), 7.57–7.62 (2H, m, Aromatic CH), 7.71–7.76 (2H, m, Aromatic C-H), 8.21 (1H, s, -CH), 10.47 (1H, s, NH), 11.67 (1H, s, NH). ^{13}C-NMR (75 MHz, DMSO-d_6): δ: 36.30, 116.30 (d, J = 21.84 Hz), 119.36, 125.87 (d, J = 3.66 Hz), 129.35, 129.59, 129.86, 131.04 (d, J = 8.08 Hz), 131.08 (d, J = 7.99 Hz), 139.70, 143.13, 163.97 (d, J = 177.48 Hz), 169.26. HRMS (m/z): $[M+H]^+$ calcd for $C_{17}H_{13}N_5OFS_2Cl$: 422.0307; found: 422.0309.

2-((5-((4-chlorophenyl)amino)-1,3,4-thiadiazol-2-yl)thio)-N′-(4-chlorobenzylidene) acetohydrazide (5f)

Yield: 84%, M.P. = 218°C. ^{1}H-NMR (300 MHz, DMSO-d_6): δ: 4.44 (2H, s, -S-CH_2), 7.35–7.38 (2H, m, -Aromatic CH), 7.45–7.48 (2H, m, Aromatic CH), 7.56–7.59 (2H, m, Aromatic CH), 7.67–7.70 (2H, m, Aromatic C-H), 8.01 (1H, s, -CH), 10.47 (1H, s, NH), 11.72 (1H, s, NH). ^{13}C-NMR (75 MHz, DMSO-d_6): δ:36.27, 119.36, 125.86, 128.99, 129.34, 133.32, 134.87, 139.68, 142.99, 146.40, 153.35, 165.18, 169.24. HRMS (m/z): $[M+H]^+$ calcd for $C_{17}H_{13}N_5OS_2Cl_2$: 438.0011; found: 438.0023.

2-((5-((4-chlorophenyl)amino)-1,3,4-thiadiazol-2-yl)thio)-N′-(4-(acetamido) benzylidene) acetohydrazide (5g)

Yield: 77%, M.P. = 231°C. ^{1}H-NMR (300 MHz, DMSO-d_6): δ: 2.09 (3H, s, CH_3),4.43 (2H, s, -S-CH_2), 7.34–7.35 (1H, m, -Aromatic CH), 7.37–7.38 (1H, m, Aromatic CH), 7.56–7.66 (6 H, m, Aromatic CH), 8.13 (1H, s, -CH), 10.09 (1H, s, NH), 10.47 (1H, s, NH), 11.57 (1H, s, NH). ^{13}C-NMR (75 MHz, DMSO-d_6): δ: 24.55, 36.34, 119.37, 125.84, 128.04, 128.33, 128.97, 129.36, 139.70, 141.38, 144.11, 153.55, 163.69, 165.09, 168.91. HRMS (m/z): $[M+H]^+$ calcd for $C_{19}H_{17}N_6O_2S_2Cl$: 461.0616; found: 461.0625.

2-((5-((4-chlorophenyl)amino)-1,3,4-thiadiazol-2-yl)thio)-N′-(4-(dimethylamino) benzylidene) acetohydrazide (5h)

Yield: 72%, M.P. = 229°C. ^{1}H-NMR (300 MHz, DMSO-d_6): δ: 2.92–2.96 (6H, s, CH_3),4.39 (2H, s, -S-CH_2), 6.67–6.75 (2H, m, -Aromatic CH), 7.35–7.39 (2H, m, -Aromatic CH), 7.43–7.46 (1H, m, Aromatic CH), 7.48–7.52 (1H, m, Aromatic CH), 7.58–7.62 (2H, m, -Aromatic CH), 8.04 (1H, s, -CH), 10.48 (1H, s, NH), 11.37 (1H, s, NH). ^{13}C-NMR (75 MHz, DMSO-d_6): δ: 36.40, 37.00, 112.20, 119.35, 121.72, 125.81, 128.62, 128.96, 129.34, 139.72, 145.08, 151.85, 163.17, 168.54. HRMS (m/z): $[M+H]^+$ calcd for $C_{19}H_{19}N_6OS_2Cl$: 447.0823; found: 447.0827.

2-((5-((4-chlorophenyl)amino)-1,3,4-thiadiazol-2-yl)thio)-N′-(4-(diethylamino) benzylidene) acetohydrazide (5i)

Yield: 71%, M.P. = 207°C. ^{1}H-NMR (300 MHz, DMSO-d_6): δ: 1.05–1.10 (6H, m, CH_3),3.34–3.38 (4H, m, CH_2),4.39 (2H, s, -S-CH_2), 6.62–6.69 (2H, m, -Aromatic CH), 7.35–7.42 (3H, m, -Aromatic CH), 7.45–7.48 (1H, m, Aromatic CH), 7.58–7.62 (2H, m, Aromatic CH), 8.02 (1H, s, -CH), 10.48 (1H, s, NH), 11.34 (1H, s, NH). ^{13}C-NMR (75 MHz, DMSO-d_6): δ: 12.86, 36.38, 44.15, 111.50, 119.34, 120.79,125.82, 128.95, 129.35, 139.72, 145.14, 149.21, 163.08, 165.06, 168.48. HRMS (m/z): $[M+H]^+$ calcd for $C_{21}H_{23}N_6OS_2Cl$: 475.1136; found: 475.1146.

Anticancer activity

The absorbance values obtained from MTT experiments were used to assess the anticancer properties of compounds 5a–5i. As previously mentioned, the MTT method was used [30]. The anticancer activities of the compounds were evaluated against 3 cancer cell lines (MCF-7, MDA and HT-29). L929 healthy mouse fibroblast cells were used to evaluate the selectivity of the compounds. In cell lines, cisplatin served as a reference drug.

Annexin V binding assay

Approximately 5×10^5 seeds of each cancer cell were seeded into 6-well plates and allowed to adhere overnight. The next day, drugs found to be effective for MCF-7, MDA and HT-29 cancer cells were incubated at IC_{50} doses for another 24 hours. Cells harvested after trypsinization were suspended in PBS containing at least 1% FBS. The manufacturer's instructions were then followed and the Annexin V & Dead Cell reagent was mixed with the cells. Afterwards, the percentage of dead, viable, early and late apoptic cells were determined using the Muse Cell Analyser (Millipore) device.

Immunoflorescent microscope analysis

The Immunofluorescent microscope analysis study was performed as mentioned in our previous work [31].

Carbonic anhydrase I/II inhibition assay

The esterase activity method is the method used for the determination of the carbonic anhydrase enzyme. With this method, esterase activity of carbonic anhydrase enzyme can be determined. Esterases responsible for the hydrolysis of carboxylic acids are capable of hydrolysing many substrates. *p*-nitrophenyl acetate is a substrate used in esterase and lipase activity assays. Hydrolysis of 1,4 *p*-nitrophenyl acetate yields *p*-nitrophenol or *p*-nitrophenolate, which gives maximum absorbance at 405 nm. The measurement is not affected because the two formed structures peak at the same absorbance value [32,33].

CA-IX ELISA test

The CA-IX ELISA assay was performed as previously described [34]. Phenol red (at a concentration of 0.2 mM) was used as indicator, working at the absorbance maximum of 557 nm, with 20 mM Hepes (pH 7.5) as buffer and 20 mM Na_2SO_4 (for maintaining constant the ionic strength), following the initial rates of the CA-catalysed CO_2 hydration reaction for a period of 10–100 s. The CO_2 concentrations ranged from 1.7 to 17 mM for the determination of the kinetic parameters and inhibition constants. For each inhibitor, at least six traces of the initial 5–10% of the reaction have been used for determining the initial velocity. Potential inhibitors and enzyme solutions were preincubated together for 6 h at room temperature prior to assay in order to allow for the formation of the E–I complex. The inhibition constants were obtained by nonlinear least-squares methods using PRISM 3 and the Cheng–Prusoff equation, as reported earlier, and represent the mean from at least three different determinations. CA IX was recombinant one obtained in house and its concentrations in the assays system were of the order of 10–12.5 nM.

Results and discussion

Chemistry

The synthesis of the title 2-((5-((4-chlorophenyl)amino)-1,3,4-thiadiazol-2-yl)thio)-*N*′-(substituted benzylidene) acetohydrazide (5a-5i) was accomplished by a synthetic procedure as illustrated in the Scheme 1 and Table 1. Mass spectrum and NMR data were used to identify every molecule that was produced. 4-chloroisothiocyanate on treatment with 99% hydrazine hydrate in the presence of ethanol yield *N*-(4-chlorophenyl)hydrazinecarbothioamide (1). The obtained compound 1 was

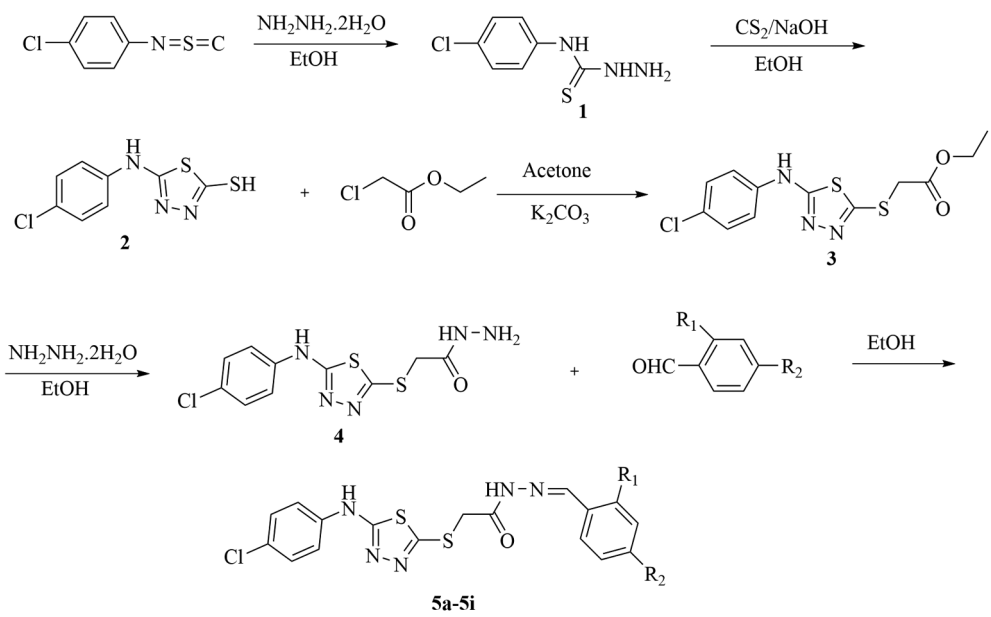

Scheme 1. General procedure for synthesis of the final compounds 5a–5i.

Table 1. Structure of synthesized compounds 5a–5i.

Comp.	*R1*	*R2*
5a	-H	-H
5b	-F	-H
5c	-Cl	-H
5d	$-OCH_3$	-H
5e	-H	-F
5 f	-H	-Cl
5 g	-H	acetamido
5 h	-H	dimethylamino
5i	-H	diethylamino

then subjected to cyclization in the following step through a reaction with carbon disulphide and NaOH in ethanol to produce 5-(4-chlorophenylamino)-1,3,4-thiadiazole-thiol (2). A mixture of compound 2 and chloroethylacetate in dry acetone with anhydrous potassium carbonate was refluxed for 8 h. To obtain 2-((5-((4-chlorophenyl)amino)-1,3,4-thiadiazol-2-yl)thio)acetohydrazide (4), compound 3 was refluxed with hydrazine hydrate in ethanol. A mixture of hydrazide derivative (4) and the appropriate benzaldehyde derivatives in EtOH was refluxed and obtained target compounds (5a–5i).

The target compounds (5a–5i)′ chemical structures were verified by ^{1}H-NMR, ^{13}C-NMR, and high-resolution mass spectrometry (HRMS) (See Supplementary material). The singlet signals at 11.34 ppm and 8.01 ppm in all of the spectra (O=C-NH) and N=CH, respectively, verified the N-acylhydrazone skeleton in the structures of compounds 5a–5i. The compounds 5a–5i's ^{1}H NMR spectrum analysis revealed that the S-CH2 (methylene) protons were detected as a singlet between 4.39 and 4.46 ppm. In the ^{1}H NMR spectra, a singlet signal at 3.84 ppm was produced by the protons of compound 5d's methoxy substituent. NH protons between thiadiazole and phenyl rings were observed as singlet in the range of 10.47–10.48 ppm.

In the ^{13}C-NMR spectrum, the signal of the methoxy group was observed at δ 56.12 ppm. The S-CH_2 (methylene) carbons were signalled between δ 4.39–4.46 ppm. ^{13}C-NMR spectra of the compounds displayed signals at around δ 165 ppm that belong to the carbonyl carbon. The measured $[M+H]^+$ values were consistent with the expected ones, according to HRMS data.

Anticancer activity

The newly developed thiadiazole-hydrazone derivatives (5a–5i) were examined for their preliminary anticancer activity against four different types of human cancer cell lines such as MCF7 (breast cancer), MDA (breast cancer), HT-29 (colon cancer), and L929 (normal fibroblast cell) by using the MTT assay and obtained results are summarized in Table 2. The chemotherapeutic anticancer drug such as cisplatin was used as a positive control. Among the investigated compounds, four compounds (5b, 5d, 5f, and 5i) display potent anticancer activity. In specific, compounds 5b and 5d show superior activity against both breast cancer cells (MCF-7, MDA) with IC_{50} values in the range of 9.19 to 24.74 μM. Furthermore, compounds 5f and 5i are promising against MCF-7 with IC_{50} values in the range of 23.50 to 31.45 μM, when compared with the cisplatin

Table 2. In vitro cytotoxicity activity of (5a–5i) with IC_{50} in μM.

Comp.	*L929*	*MCF7*	*MDA*	*HT-29*
5a	>100	>100	>100	>100
5b	67.84	9.19	15.27	78.65
5c	>100	>100	>100	>100
5d	>100	24.74	10.43	>100
5e	87.87	>100	>100	>100
5f	>100	31.45	>100	68.41
5g	>100	>100	>100	>100
5h	99.4	>100	>100	99.78
5i	>100	23.50	>100	>100
Cisplatin	44.9	31.45	36.9	78.7

(IC_{50} = 31.45 μM). Compounds 5b (78.65 μM) and 5f (68.41 μM) are the most active compounds against HT-29 cell line. Chemotherapy's toxicity towards healthy cells is a major barrier to effective cancer treatment. It is notable that our chemicals show selectivity between cancer cell lines and healthy cell lines. When the IC_{50} values of the compounds against the healthy cell line (L929) were examined, it was seen that the selectivities of the compounds were high.

When the cytotoxicity data were analysed in terms of the chemical structures of the compounds, it was noticed that the presence of fluorine substituent in the *ortho* position of the phenyl ring (compound 5b) increases the anticancer activity, while the activity decreases significantly with the fluorine substituent turning into the *para* position (compound 5e). The presence of the methoxy group in the 2nd position of the phenyl ring (compound 5d) increases the activity against the MCF-7 cell line. It was determined that while the fluorine substituent in the para position (compound 5e) decreases the activity against MCF-7, the presence of chlorine atom increases the activity (compound 5f). While the presence of dimethyl amino group in the para position of the phenyl ring decreases the activity, it is seen that the anticancer activity increases with the elongation of the alkyl chain (diethylamino).

Annexin V binding assay

The IC_{50} doses obtained for each cancer cell line as a result of MTT were determined. By using these doses, the death pathways of the active synthesis structures on the cells were determined by flow cytometry. Each result found was compared with the results obtained in the presence of cisplatin. Each active new synthesis structure showed almost the same effect as cisplatin with IC_{50} doses and enabled cancerous cells to undergo early apoptosis in a desired manner.

According to the MTT assay, compounds 5b, 5d, 5f, 5i for MCF-7 cell line; compounds 5b, 5d for MDA cell line; compound 5f for HT-29 cell line were selected for the flow cytometric analysis. Flow cytometric analysis diagram of cisplatin with compounds 5b, 5d, 5f and 5i in MCF-7 cell line is presented in Figure 2. Compound 5f causes the highest percentage of apoptosis (early + late apoptotic cells) with 58.45% whereas cisplatin causes 46.50% on MCF-7 cells. The other compounds namely 5b, 5d and 5i possess 47.6, 47.15 and 49.3% apoptotic cell percentages.

For MDA cell line, the percentage of apoptotic cells at IC_{50} concentrations was calculated as 47.65% for cisplatin and 49.3% for compound 5b, 47.7% for compound

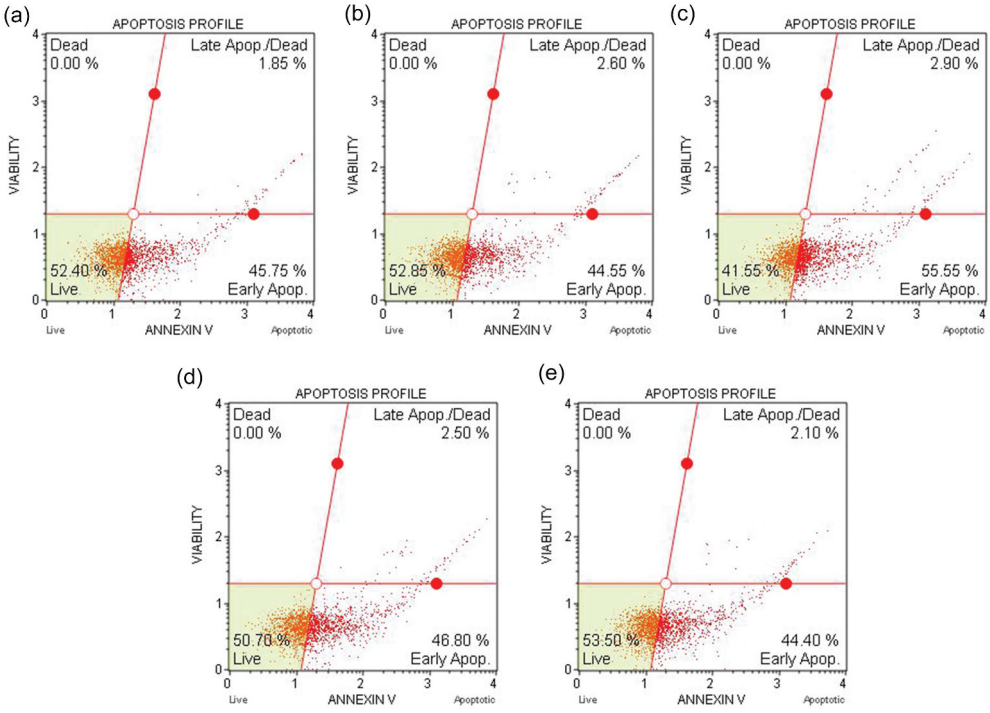

Figure 2. Flow cytometry results for compounds 5b (a), 5d (b), 5f (c), 5i (d) and cisplatin (e) for mcf-7 cell line.

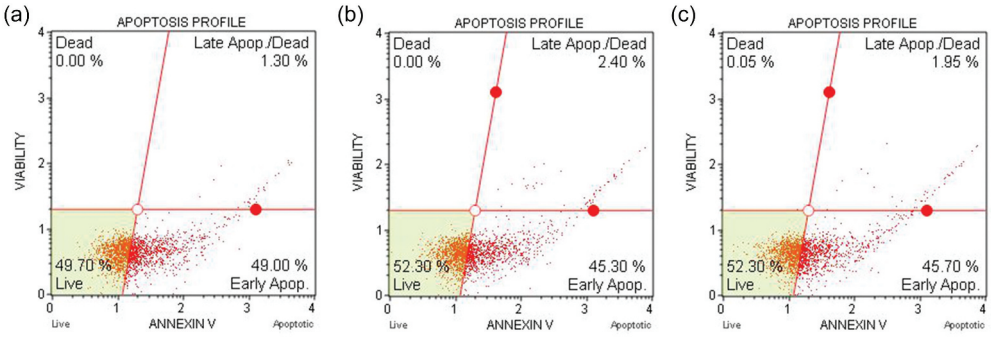

Figure 3. Flow cytometry results for compounds 5b (a), 5d (b) and cisplatin (c) for MDA.

5d (Figure 3). Flow cytometric analysis diagram of cisplatin with compound 5f is presented in Figure 4 for HT-29 cell line. Accordingly, the percentage of apoptotic cells at IC_{50} concentrations was calculated as 46.25% for cisplatin and 45.5% for compound 5f.

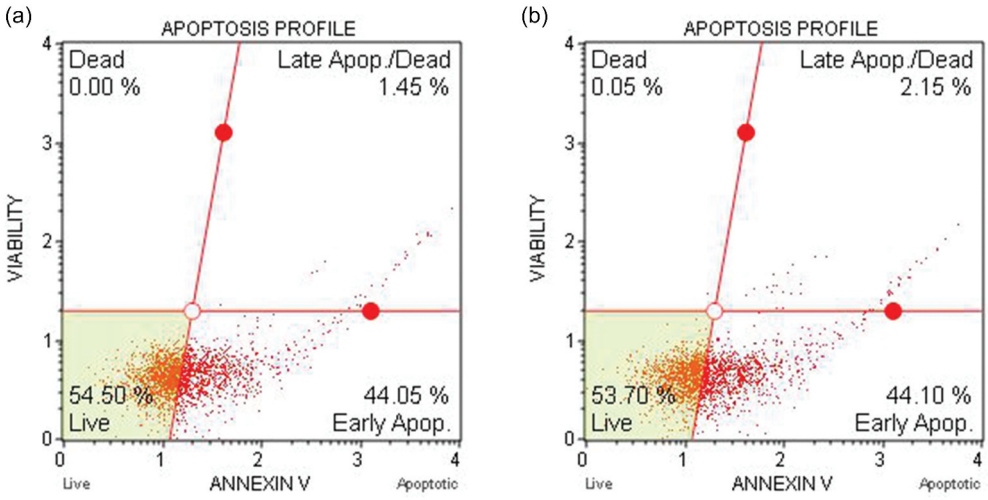

Figure 4. Flow cytometry results for compounds 5f (a) and cisplatin (b) for HT-29.

Immunoflorescent microscope analysis

Fluorescent staining degrees of HT29, MDA, and MCF cancer cell lines labelled with cell cycle arresting p21 antibody and immunofluorescence technique were compared light microscopically. Accordingly, compound 5f, control, and cisplatin were applied to the cell lines and kept for 24 hours. The p21 immunolocalization of the compound 5f groups in HT29 colon cancer cells was compared with the control and cisplatin groups. Accordingly, high p21 immunolocalization was seen in compound 5f. (Figures S1–S2 in Supplementary material).

The p21 immunolocalization of compound 5b in MCF-7 breast cancer cells was compared with the control and cisplatin groups. Accordingly, high p21 immunolocalization was seen in compound 5b (Figures S3–S4 in Supplementary material).

The p21 immunolocalization of the compound 5d in MDA breast cancer cells was compared with the control and cisplatin groups. Accordingly, high p21 immunolocalization was seen in compound 5d (Figures S5–S6 in Supplementary material).

Carbonic anhydrase I, II and IX inhibition assay

Our synthetic structures were investigated using the esterase assay method with two physiologically relevant isoenzyme carbonic anhydrases. Among these enzymes, carbonic anhydrase-I (hCA I) has a slower cytosolic isoform and carbonic anhydrase-II (hCA II) has a faster inhibition potential. Inhibition data of the compounds against hCA I and hCA II isoforms are summarized in Table 3 and Figure S7 (in Supplementary material). CA-IX Elisa test results are given in Figure 5. While compounds 5 g and 5i did not have an inhibitory effect, it was determined that compound 5d had a high inhibitory effect on hCA I and compound 5b had a high inhibitory effect on hCA II. The obtained results were compared with Acetazolamide used as a standard. Based on these results, it was determined that

Table 3. IC_{50} (μM) values against hCA I and hCA II enzymes.

	IC_{50} (μM)			
Comp.	*hCA I*	r^2	*hCA II*	r^2
5a	42.33	0.9692	70.71	0.8420
5b	68.15	0.8317	23.18	0.9782
5c	84.10	0.8259	46.03	0.9284
5d	29.74	0.9308	48.95	0.9364
5e	47.23	0.9110	39.5	0.9536
5f	82.21	0.8649	38.93	0.9222
5g	-	-	-	-
5h	99.9	0.7572	116.9	0.8231
5i	-	-	-	-
AZA*	28.11	0.9387	35.65	0.9756

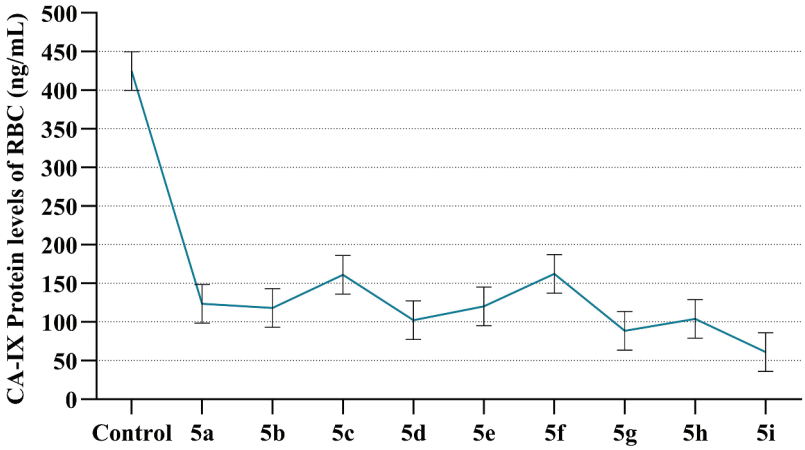

Figure 5. Comparison of hCA IX concentrations against each compound.

compounds 5b and 5d could be used as an alternative carbonic anhydrase inhibitor. Among them, compound 5d exhibited remarkable hCA I inhibitory activities compared to a standard inhibitor, with IC_{50} values in the range of 29.74 μM. It was determined that the presence of fluoro substituent, which is an electron withdrawing group, increases the effect on hCA II, while the methoxy group, which is an electron donating group, increases the activity on hCA I. When the effect of compounds on CA-IX Protein level at 40 μl concentration was examined, it was found that compound 5i had the highest efficiency.

Molecular docking

Docking simulation were performed by using AutoDock VINA integrated in the PyRx 0.8 [35] virtual screening tool to identify compounds with high binding affinity.

In silico docking simulation studies to evaluate the molecular interactions of compounds 5b and 5d were done with the human carbonic anhydrase I and II (CA I and II) proteins which were retrieved from the protein data bank with the PDB ID:6G3V (hCA I) and 6G3Q (hCA II) and these proteins have a co-crystallized famotidine as an antagonist ligand. Protein structures were processed to ensure an optimized structure for docking

studies and it was executed with UCSF Chimera Dock Prep module and that includes the following steps: elimination of water molecules and other ligands, addition of missing atoms and residues, energy minimization and assigning charges and polar hydrogens and then converted to the pdbqt format.

The 2D structure of the ligands was drawn with ChemDraw software and the structures were optimized through energy minimization with MMFF94 force field parameters and conjugate gradient algorithm using Open Babel module of PyRx and eventually converted the ligands to the AutoDock compatible pdbqt format to carry out docking exploration.

Post docking analysis and visualization of binding poses and molecular interactions were done with BIOVIA Discovery Studio 2021 and Chimera X tools [36].

Binding energies and molecular interaction profile of the compounds were compared with the acetazolamide which is a standard compound used for the in vitro activity and famotidine which is a co-crystallized ligand with the protein structures of carbonic anhydrase I and II.

Binding affinity outcomes obtained from the docking assessments are shown in Figure S8 (Supplementary material).

Molecular interaction profile of compounds 5b and 5d with carbonic anhydrase I

Compound 5d is displaying two H-bonds with the active site residues THR199 (3.61 Å) and GLN92 ((3.99 Å) where the -Cl on the phenyl ring has an interaction with THR199 and the –NH group linking with the five membered thiadiazole ring has another hydrogen bond interaction with GLN92 amino acid residue. LEU198 had a pi-sigma interaction with the halogen (-Cl) substituted phenyl ring at one of the terminals where it also exhibits pi-pi T-shaped interaction with HIS94. It has pi-alkyl and alkyl interactions with HIS119, VAL62, TRP209 ALA121, sulphur in the thiadiazole ring has a pi-sulphur interaction with PHE91 and van der Waals interactions with the remaining active site amino acids and zinc ion.

Compound 5b has one H-bond with THR199 (3.62 Å) through the -Cl substituted on the phenyl ring and this similar interaction is also found with the compound 5d. It has a pi-sigma interaction with LEU198, pi-pi-T shaped interaction with HIS94, pi-alkyl interactions with ALA121, HIS119, TRP209, VAL143 and VAL62, pi-sulphur interaction with PHE91 and a halogen (-F) interaction with HIS64 and then van der Waals interactions with the other residues in the close proximity.

Acetazolamide has two hydrogen bonds with THR199 (2.90 Å) and GLN92 (5.21 Å) residues like compound 5d. The -C=O of the acetamide that is linked to the thiadiazole ring has a H-bond with GLN92 and -NH of the sulfamoyl has another H-bond with THR199. Pi-sulphur interaction with the sulfamoyl group is observed with HIS200 and the same residue is also involved in the pi-pi stacked interaction. There are also pi-alkyl interactions with LEU198, ALA121, metal-acceptor interactions with the Zinc ion and van der Waals interactions with HIS119, TRP209, HIS96, LEU131, HIS67, VAL143 and PHE91.

Famotidine displays two hydrogen bond interactions with THR199 (3.17 and 4.11 Å) and HIS200 (3.19 Å). The -NH of the sulfamoyl has H-bond with THR199 and -S=O of the same group has interaction with both HIS200 and THR199 and it also has a pi-sulphur interaction with HIS96. Pi-alkyl interactions are observed with ALA135, LEU131, HIS67,

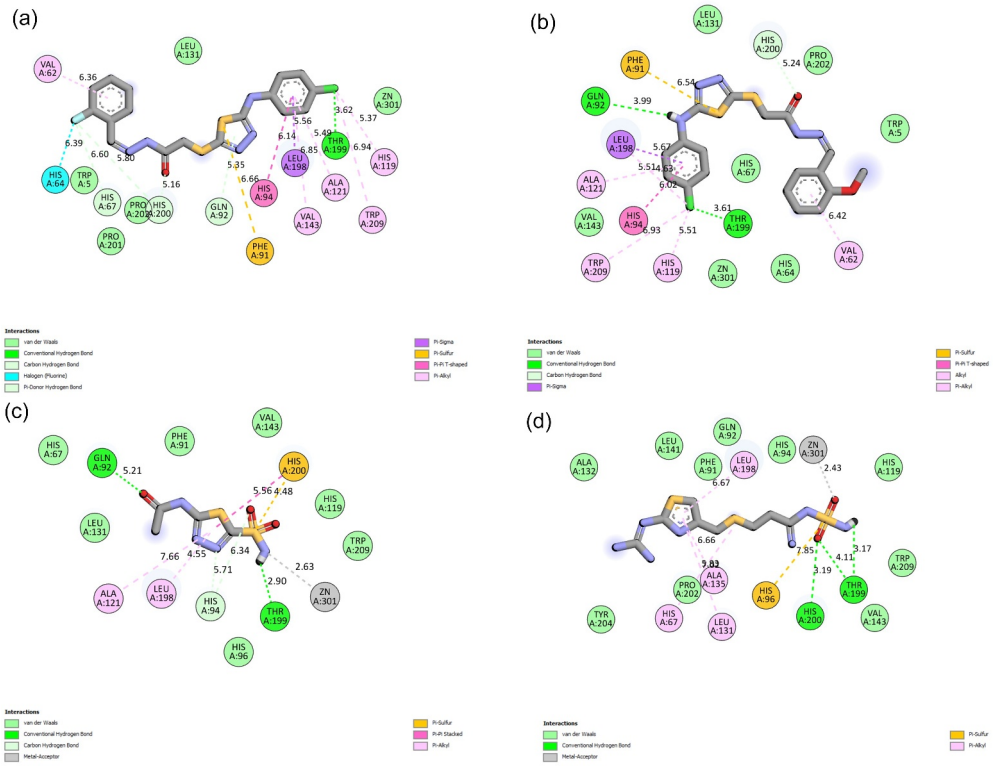

Figure 6. 2D representation of the molecular interactions of compounds 5b (a), 5d (b), Acetazolamide (c) and Famotidine (d) with the active site amino acid residues of the human carbonic anhydrase I. Interactions were displayed as colour coded dashed lines, green lines indicate the H–bonds.

LEU198 and metal -acceptor interactions with zinc ion and then van der Waals interactions with remaining active site residues (Figure 6).

Overall, the compound 5d has a better binding energy and interaction profile and the distinct biding modes of compounds 5b and 5d in the human carbonic anhydrase I active site pocket can be viewed form Figure 7.

Molecular interaction profile of compounds 5b and 5d with hCA II

Compound 5b exhibits four hydrogen bond interactions with the residues THR199 (4.00 Å), THR200 (5.02 Å), ASN67 (5.43 Å) and GLN92 (5.90 Å). The -C=O of the acetamide attached to the sulfanyl has a hydrogen bond interaction with THR199, the sulphur of the thiadiazole ring has another H-bond with THR200 and then the remaining two H-bonds are with ASN67 and GLN92 which were contributed through the interaction with the fluoro substituent on the phenyl ring of the compound 5b. Pi-cation interaction with the HIS94, alkyl and pi-alkyl interactions with LEU198, PRO202, LEU204, VAL135, metal -acceptor interaction with zinc ion and then finally van der Waals interactions with the remaining surrounding active site residues is observed.

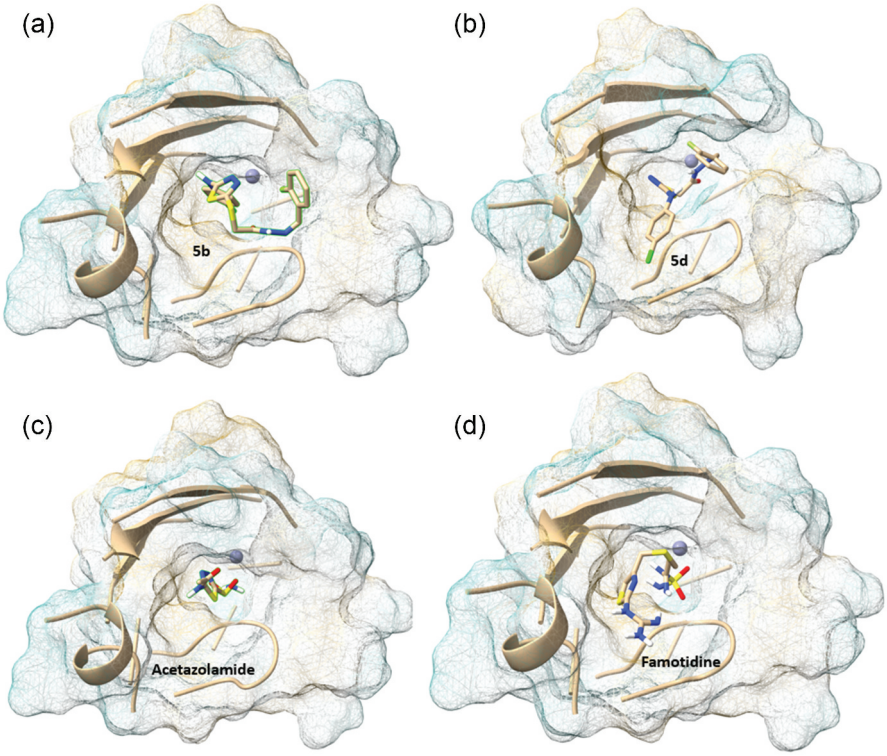

Figure 7. Binding poses of compounds 5b (a), 5d (b), Acetazolamide (c) and famotidine (d) in the active site pocket of the human carbonic anhydrase I.

Compound 5d displays two hydrogen bond interactions with THR200 (4.16 Å) and ASN62 (5.08 Å) residues. Similar H-bond interactions with THR199 through the -C=O of the acetamide attached to the sulfanyl group is found with compound 5b and the sulphur of the thiadiazole has another H-bond interaction with ASN62. The $-OCH_3$ substituted phenyl group is contributing with various other types of interactions like pi-alkyl and alkyl interactions with PHE131, LEU141, LEU198, VAL121 and VAL143, pi-cation interaction with zinc ion, pi-pi T-shaped interaction with HIS94 and it is also involved in the pi-sulphur interaction with the sulpur of the sulfanyl moiety, other pi-sulphur interaction is between the sulphur of the thiadiazole ring and TRP5 residue. Pi-sigma interaction with the chloro phenyl group is observed with TYR7 and other active site residues has van der Waals interactions (Figures 8 and 9).

Acetazolamide has two H-bond interactions with THR200 (4.29 Å) and THR199 (4.06 Å) where the acetamide moiety is contributing one H-bond through the -C=O group and another H-bond with THR199 is contributed by the sulfamoyl group and the same group is also involved in the pi-sulphur interaction with HIS94 and also a metal-acceptor interaction with zinc ion is observed along with the van der Waals interactions with the remaining active site residues.

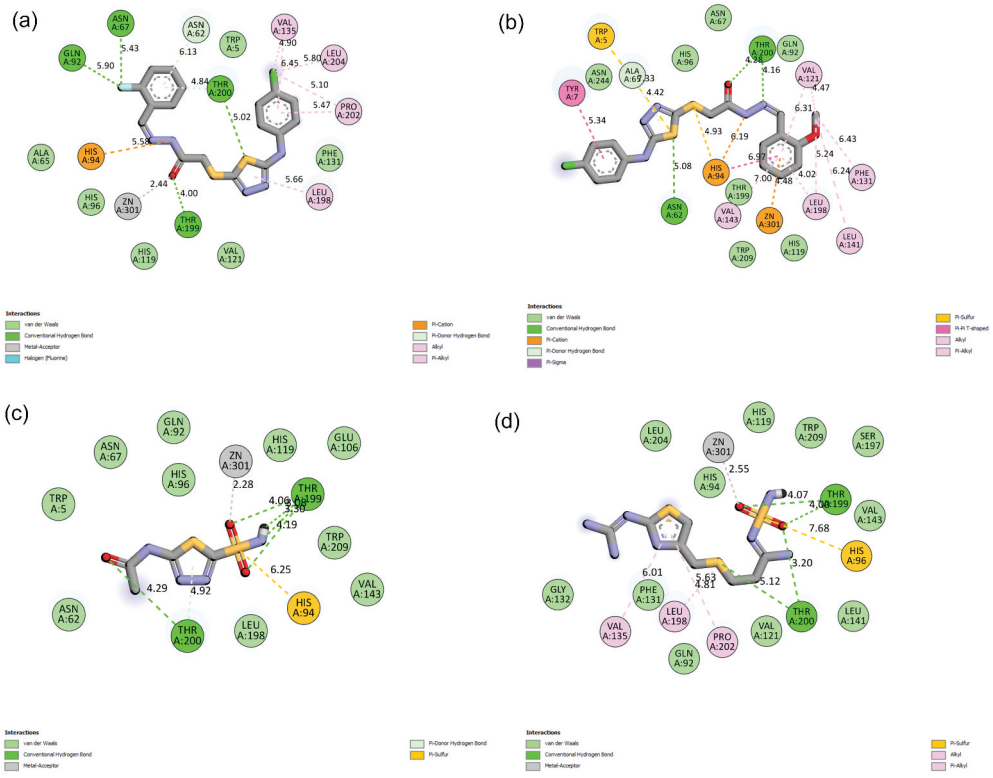

Figure 8. 2D representation of the molecular interactions of compounds 5b (a), 5d (b), Acetazolamide (c) and famotidine (d) with the active site amino acid residues of the human carbonic anhydrase II. Interactions were displayed as colour coded dashed lines, green lines indicate the H–bonds.

Famotidine has a H-bond interaction profile similar to acetazolamide where the -S=O of the sulfamoyl group is displaying two hydrogen bonding interactions with THR199 (4.00 Å) and THR200 (3.20 Å). There are also other types of interactions like pi-sulphur interactions with HIS96, pi-alkyl and alkyl interactions with PRO202, LEU198 and VAL135 and metal -acceptor interactions with zinc ions and then majority of the other residues in the active site are interacting through the van der Waals interactions.

Binding modes of the compounds 5d, 5b, Acetazolamide and Famotidine are represented in Figure 10 and the compound 5d has a distinct binding mode where the it is orienting towards a side pocket whereas the other compounds are projected towards the deeper pocket of the hCA II active site.

In carbonic anhydrase I, the -Cl substituent on the phenyl group of both the compounds 5b and 5d has a H-bond interaction with THR199 where as in the carbonic anhydrase II the -C=O in the acetamide of compounds 5b and 5d and the –S=O of the sulfamoyl groups of acetazolamide and famotidine has a similar H-bond with the THR199 and this a conserved interaction among these compounds in both the proteins.

The comparison of molecular interactions and binding poses of compounds 5b and 5d with the co-crystallized ligand (Famotidine) and Acetazolamide indicates that these compounds have a comparable interaction and binding orientation pattern (5b in hCA II and 5d

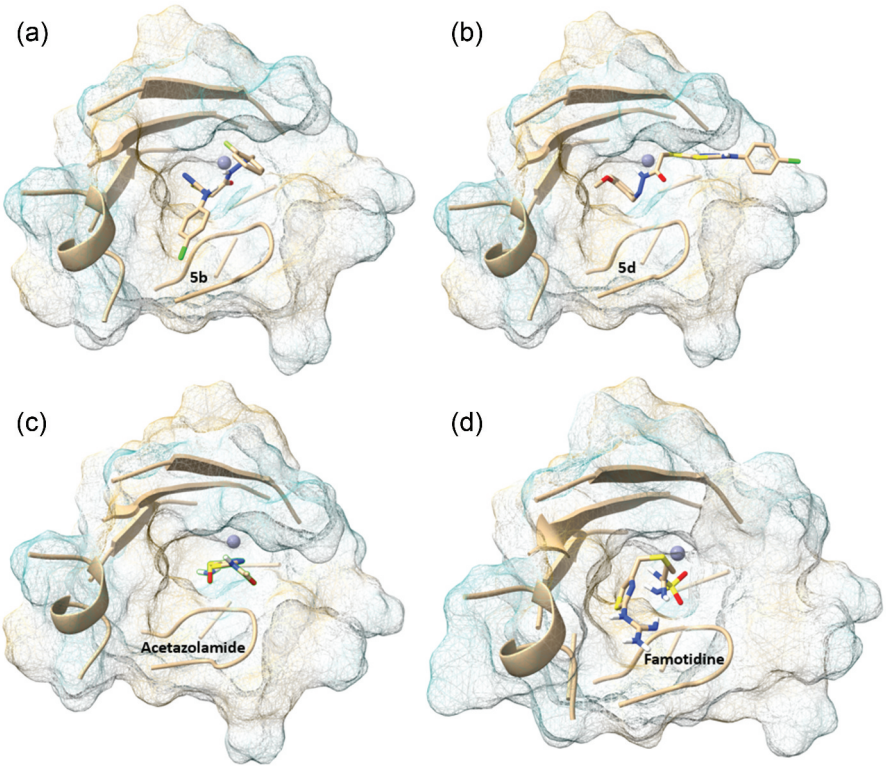

Figure 9. Binding poses of compounds 5b (a), 5d (b), Acetazolamide (c) and Famotidine (d) in the active site pocket of the human carbonic anhydrase II.

in hCA I respectively) and a similar H-bond interaction with active site residue like THR199 [35] is crucial as this could disrupt its interaction with GLU106 residue which is a critical interaction for maintaining the structural integrity of the loop in the catalytic active site of human carbonic anhydrase and by displaying this interaction compounds 5b and 5d could mimic the antagonists and various other interactions could also stabilize their binding in the active site and eventually this might be getting reflected as a better in vitro activity against hCA I and hCA II for these compounds.

Molecular docking of compound 5i with human carbonic anhydrase IX

Molecular docking studies were performed using the Human CA IX protein (PDB ID: 5FL6) to evaluate the interaction between compound 5i and the protein. Compound 5i demonstrated better CA IX inhibitory compared to the other screened compounds so it was chosen as a potential hit compound for the present docking simulations.

Compound 5i has a binding energy of −7.2 Kcal/mol and displays two H-bonds with the active site residues THR201 (4.79 Å) and ARG129 ((5.96 Å). The nitrogen in the five membered thiadiazole ring has a H-bond interaction with THR201 and the -C=O of the acetamide moiety adjacent to the sulfanyl group has another H-bond interaction with ARG129 active site residue. The -Cl substituent on the phenyl ring is involved in several

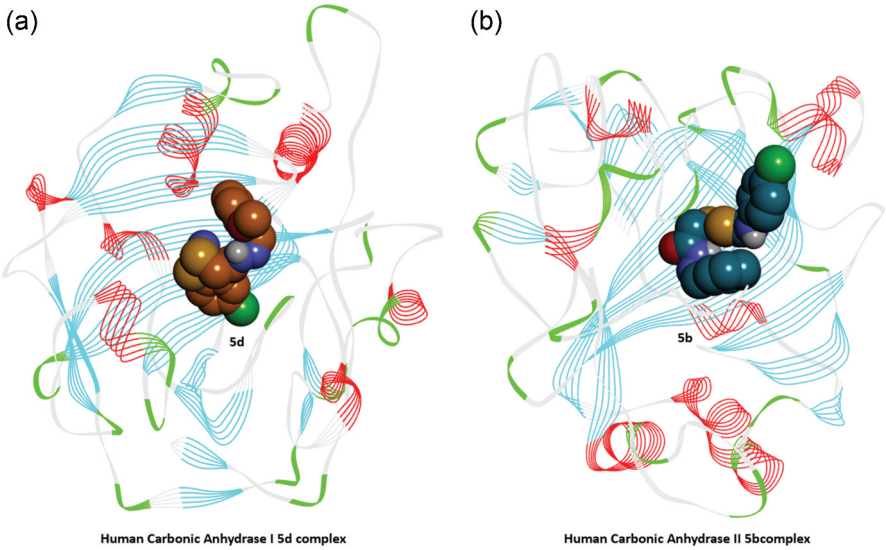

Figure 10. Human carbonic anhydrase I-5d (A) complex and human carbonic anhydrase II-5b (B) complex.

alkyl interactions with VAL142, HIS119, TRP210, VAL121 and HIS94 residues. LEU199 has a pi-sigma interactions with halogen substituted aromatic ring and the diethyl amino substituted aromatic ring has a pi-alkyl interaction with VAL130 residue. Zinc ion and the remaining residues that include CYS204, ASP131, LEU134, PRO203, GLN71, GLN92, THR200, PRO202 are in the close proximity which has a van der Waals interactions with the compound 5i.

Binding orientations of compound 5i in the active site pocket indicate that the chloro substituted amino group is projected towards the deeper position of the pocket followed by the thiadiazole, sulfanyl and acetamido localized in the pocket whereas the diethyl amino substituted phenyl methylene amino group oriented in the outer periphery of the pocket.

Compound 5i has a comparable interaction profile with the CA IX inhibitors like acetazolamide, with a similar critical H-bond interaction with THR201 by the thiadiazole nitrogen in both compounds [37].

Molecular interaction profile and the biding orientation of compound 5i in the human carbonic anhydrase IX active site pocket can be viewed form the Figures 11, 12 and 13, respectively.

ADME properties

ADME property estimation of compounds 5i, 5b and 5d with the best anticancer and carbonic anhydrase I/II inhibition were performed from SwissADME webserver (http://www.swissadme.ch/) [38].

In silico predictions for the assessment of their ADME properties were done and observed that the Lipinski drug likeness of the compounds are in compliance with

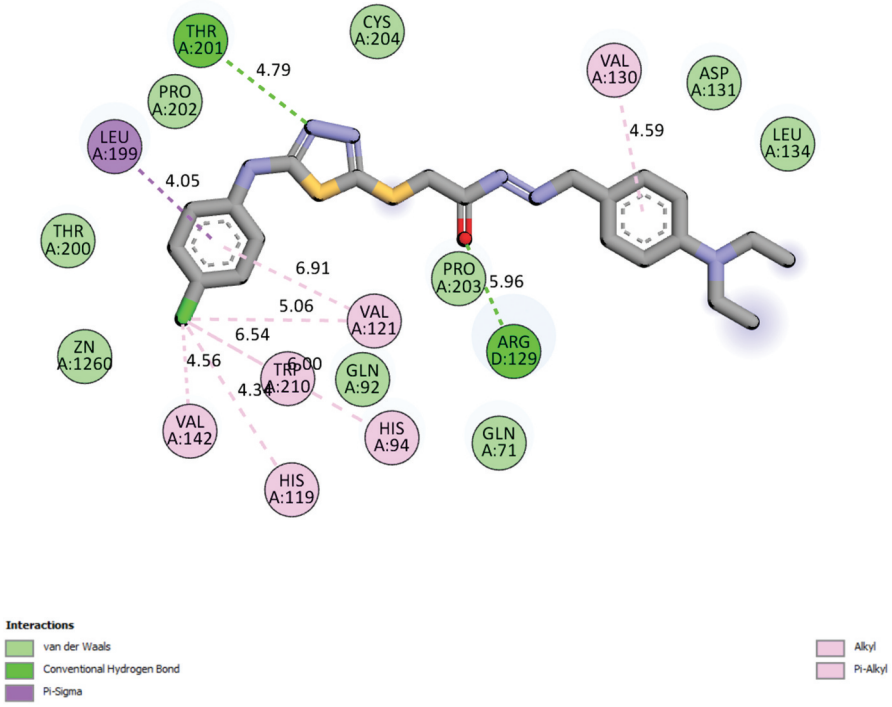

Figure 11. 2D representation of the molecular interactions of compound 5i with the active site amino acid residues of the human carbonic anhydrase IX. Interactions were displayed as colour coded dashed lines, green lines indicate the H–bonds.

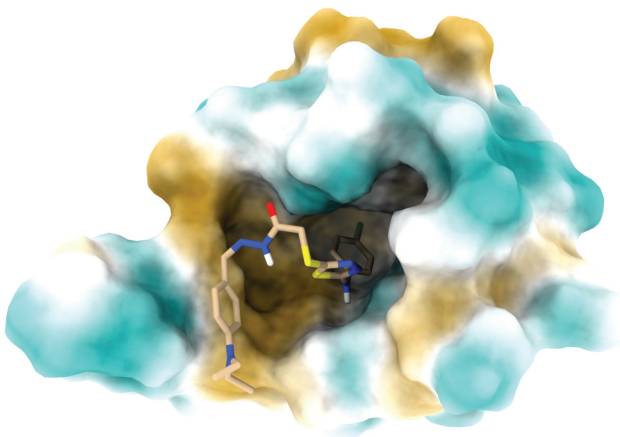

Figure 12. Binding poses of compound 5i in the active site pocket of the human carbonic anhydrase IX.

no deviations. No BBB permeation and P-glycoprotein substrate activity were predicted for these compounds. Regarding the metabolism, CYP1A2/2C19/2C9/3A4 are the isoforms inhibited by these compounds. Pharmacokinetic properties like GI absorption are low for compounds 5d and 5b therefore further

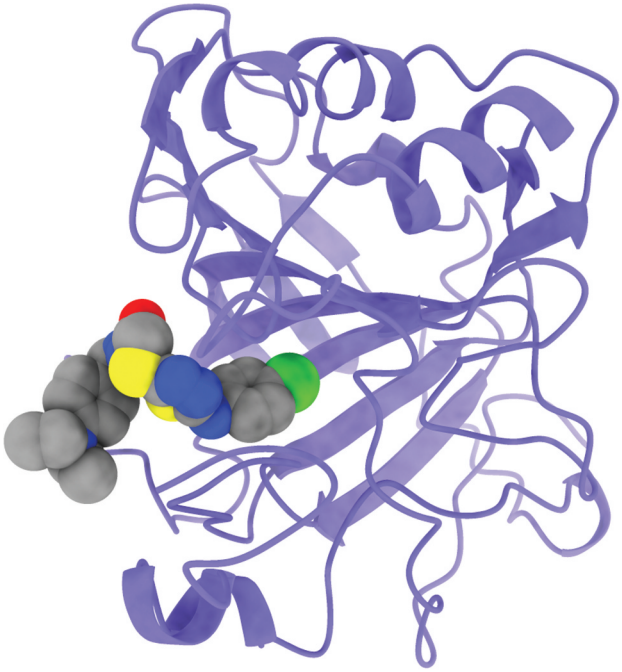

Figure 13. Protein ligand complex of compound 5i in the active site of the human carbonic anhydrase IX protein.

optimizations are required to enhance the pharmaceutical properties in the future studies (Table 4).

Overall, the compound 5i is in compliance with the Lipinski drug likeness with no deviations. No BBB permeation and P-gp substrate activity was observed. CYP2C19/2C9/3A4 are the isoforms predicted to be inhibited by compound 5i. Additional improvements are needed in future research to enhance the pharmaceutical properties of compound 5i, as the GI absorption is low and the solubility is inadequate and these ADME properties are represented in the Table 4.

Table 4. Physicochemical properties and drug-likeness predictions of compounds with better in vitro and in silico performance using SwissADME [32].

Parameters	*Compound 5b*	*Compound 5d*	*Compound 5i*
Molecular Weight (g/mol)	42,491.200	4433.9303	42,475.030
log Po/w	4.13	3.88	4.48
No. of H-bond Donors	2	2	2
No. of H-bond Acceptors	5	5	4
Solubility	Poor	Poor	Poor
TPSA	132.81 $Å^2$	142.04 $Å^2$	136.05 $Å^2$
GI absorption	Low	Low	Low
BBB permeation	No	No	No
P-gp substrate	No	No	No
Drug likeness (Lipinski)	Yes	Yes	Yes
Bioavailability score	0.55	0.55	0.55
CYP450 isoforms inhibition	CYP1A2/2C19/2C9/3A4	CYP1A2/2C19/2C9/3A4	CYP2C19/2C9/3A4

Conclusion

In this study, two potent pharmacophores thiadiazole and hydrazone were combined in one molecule and a series of thiadiazole-hydrazone was synthesized. These compounds were screened against three cancer cell lines healthy cell line as well as hCA I, II and IX. Compound 5d showed higher inhibitory activity compared to standard inhibitors with an IC_{50} value of 29.74 for hCA I, and compound 5b showed the most activity with an IC_{50} value of 23.18 for hCA II. Also, compound 5i was found to have the highest activity for the CA IX enzyme. In addition, these compounds showed the highest anticancer effect in the series. An Annexin V study on active compounds showed that it could induce cancer cell apoptosis. Overall compounds 5d and 5b had a better binding and molecular interaction profile against their respective targets and these compounds could be further explored as a promising lead compound against the carbonic anhydrase target.

Cancer cells often show programmed proliferation and migration. Abnormal expression of many cell cycles and apoptotic proteins refers to the biological characteristics of cancer cells. Basically, kinases are responsible for altering the cell cycle by dysregulating different checkpoints; their inhibition regulates the cell cycle, leading to apoptosis and inhibition of cancer cell migration. Therefore, kinases are a potential therapeutic target for cancer cells. Determination of p53 and its dependent p21 expression in today's common cancer types such as colon and breast cancer bring new perspectives to treatment approaches [39]. The p21 localization found in addition to cytotoxicity and apoptosis assays of the compound 5f component in the HT29 cell line, the compound 5b component in the MCF7 cell line, and the compound 5d component in the MDA cell line confirm the anticancer activity of these compounds in cancer cells.

Disclosure statement

No potential conflict of interest was reported by the author(s).

Funding

The author(s) reported there is no funding associated with the work featured in this article.

References

[1] M. Tapera, H. Kekeçmuhammed, B. Tüzün, E. Sarıpınar, Ü.M. Koçyiğit, E. Yıldırım, M. Doğan, and Y. Zorlu, *Synthesis, carbonic anhydrase inhibitory activity, anticancer activity and molecular docking studies of new imidazolyl hydrazone derivatives*, J. Mol. Struct. 1269 (2022), pp. 133816. doi:10.1016/j.molstruc.2022.133816.

[2] S. Bilginer, S.K. Bardaweel, Y. Demir, I. Gulcin, and C. Kazaz, *Synthesis, cytotoxicities, and carbonic anhydrase inhibition activities of pyrazoline–benzenesulfonamide derivatives harboring phenol/polyphenol moieties*, Med. Chem. Res. 31 (2022), pp. 925–935. doi:10.1007/s00044-022-02893-z.

[3] V. Chahal and R. Kakkar, *A combination strategy of structure-based virtual screening, MM-GBSA, cross docking, molecular dynamics and metadynamics simulations used to investigate natural compounds as potent and specific inhibitors of tumor linked human carbonic anhydrase IX*, J. Biomol. Struct. Dyn. 41 (2023), pp. 5465–5480. doi:10.1080/07391102.2022.2087736.

[4] H.O. Tawfik, M.A. Shaldam, A. Nocentini, R. Salem, H. Almahli, S.T. Al-Rashood, C.T. Supuran, and W.M. Eldehna, *Novel 3-(6-methylpyridin-2-yl) coumarin-based chalcones as selective inhibitors of cancer-related carbonic anhydrases IX and XII endowed with anti-proliferative activity*, J. Enz. Inhib. Med. Chem. 37 (2022), pp. 1043–1052. doi:10.1080/14756366.2022.2056734.

[5] H.O. Tawfik, A. Belal, M.A. Abourehab, A. Angeli, A. Bonardi, C.T. Supuran, and M.H. El-Hamamsy, *Dependence on linkers' flexibility designed for benzenesulfonamides targeting discovery of novel hCA IX inhibitors as potent anticancer agents*, J. Enz. Inhib. Med. Chem. 37 (2022), pp. 2765–2785. doi:10.1080/14756366.2022.2130285.

[6] A. Bonardi, S. Bua, J. Combs, C. Lomelino, J. Andring, S.M. Osman, A. Toti, L.D.C. Mannelli, P. Gratterib, C. Lomelinoc, R. McKenna, A. Nocentini, and C.T. Supuran, *The three-tails approach as a new strategy to improve selectivity of action of sulphonamide inhibitors against tumour-associated carbonic anhydrase IX and XII*, J. Enz. Inhib. Med. Chem. 37 (2022), pp. 930–939. doi:10.1080/14756366.2022.2053526.

[7] A.I. Zain-Alabdeen, T.F. El-Moselhy, N. Sharafeldin, A. Angeli, C.T. Supuran, and M.H. El-Hamamsy, *Synthesis and anticancer activity of new benzensulfonamides incorporating s-triazines as cyclic linkers for inhibition of carbonic anhydrase IX*, Sci. Rep. 12 (2022), pp. 16756. doi:10.1038/s41598-022-21024-7.

[8] A. Kumar, K. Siwach, C.T. Supuran, and P.K. Sharma, *A decade of tail-approach based design of selective as well as potent tumor associated carbonic anhydrase inhibitors*, Bioorg. Chem. 126 (2022), pp. 105920. doi:10.1016/j.bioorg.2022.105920.

[9] G. Arrighi, A. Puerta, A. Petrini, F.J. Hicke, A. Nocentini, M.X. Fernandes, J.M. Patron, C. T. Supuran, J.G. Fernández-Bolaños, and Ó. López, *Squaramide-tethered sulfonamides and coumarins: Synthesis, inhibition of tumor-associated cas ix and xii and docking simulations*, Int. J. Mol. Sci. 23 (2022), pp. 7685.

[10] H.O. Tawfik, A. Petreni, C.T. Supuran, and M.H. El-Hamamsy, *Discovery of new carbonic anhydrase IX inhibitors as anticancer agents by toning the hydrophobic and hydrophilic rims of the active site to encounter the dual-tail approach*, Eur. J. Med. Chem. 232 (2022), pp. 114190. doi:10.1016/j.ejmech.2022.114190.

[11] T. Al-Warhi, M.M. Elbadawi, A. Bonardi, A. Nocentini, A.A. Al-Karmalawy, N. Aljaeed, O. J. Alotaibi, H.A. Abdel-Aziz, C.T. Supuran, and W.M. Eldehna, *Design and synthesis of benzothiazole-based SLC-0111 analogues as new inhibitors for the cancer-associated carbonic anhydrase isoforms IX and XII*, J. Enz. Inhib. Med. Chem. 37 (2022), pp. 2635–2643. doi:10.1080/14756366.2022.2124409.

[12] L. Micheli, L. Testai, A. Angeli, D. Carrino, A. Pacini, F. Margiotta, L. Flori, C.T. Supuran, V. Calderone, C. Ghelardini, and L.D.C. Mannelli, *Inhibitors of mitochondrial human carbonic anhydrases VA and VB as a therapeutic strategy against paclitaxel-induced neuropathic pain in mice*, Int. J. Mol. Sci. 23 (2022), pp. 6229. doi:10.3390/ijms23116229.

[13] D.M. Elimam, W.M. Eldehna, R. Salem, A. Bonardi, A. Nocentini, S.T. Al-Rashood, M.M. Elaasser, P. Gratteri, C.T. Supuran, and H.A. Allam, *Natural inspired ligustrazine-based SLC-0111 analogues as novel carbonic anhydrase inhibitors*, Eur. J. Med. Chem. 228 (2022), pp. 114008. doi:10.1016/j.ejmech.2021.114008.

[14] B.D. Vanjare, N.G. Choi, Y.S. Eom, H. Raza, M. Hassan, K.H. Lee, and S.J. Kim, *Synthesis, carbonic anhydrase inhibition, anticancer activity, and molecular docking studies of 1,3,4-oxadiazole derivatives*, Mol. Divers. 27 (2023), pp. 193–208. doi:10.1007/s11030-022-10416-6.

[15] Ö. Güleç, C. Türkeş, M. Arslan, Y. Demir, Y. Yeni, A. Hacımüftüoğlu, E. Ereminsoy, Ö. İ. Küfrevioğlu, and Ş. Beydemir, *Cytotoxic effect, enzyme inhibition, and in silico studies of some novel N-substituted sulfonyl amides incorporating 1, 3, 4-oxadiazol structural motif*, Mol. Divers. 26 (2022), pp. 2825–2845. doi:10.1007/s11030-022-10422-8.

[16] N. Chu, Y. Wang, H. Jia, J. Han, X. Wang, and Z. Hou, *Design, Synthesis and biological evaluation of new carbohydrate-based coumarin derivatives as selective carbonic anhydrase ix inhibitors via "click" reaction*, Molecules 27 (2022), pp. 5464. doi:10.3390/molecules27175464.

[17] M.A. Abdelgawad, S.N. Bukhari, A. Musa, M. Elmowafy, M.H. Elkomy, A.A. Nayl, A.H. El-Ghorab, I. O. Althobaiti, H.A. Altaleb, H. Omar, A.H. Abdelazeem, M.A. Zaki, M.E. Shaker, and H.A. H. Elshemy, *New sulfamethoxazole derivatives as selective carbonic anhydrase ix and xii inhibitors: Design, synthesis, cytotoxic activity and molecular modeling*, Pharm. 15 (2022), pp. 1134.

[18] B. Zengin Kurt, G. Celebi, D. Ozturk Civelek, A. Angeli, A. Akdemir, F. Sonmez, and C. T. Supuran, *Tail-approach-based design and synthesis of coumarin-monoterpenes as carbonic anhydrase inhibitors and anticancer agents*, ACS Omega 8 (2023), pp. 5787–5807. doi:10.1021/acsomega.2c07459.

[19] S. Bondock, T. Albarqi, T. Nasr, N.M. Mohamed, and M.M. Abdou, *Design, synthesis, cytotoxic evaluation and molecular docking of novel 1,3,4-thiadiazole sulfonamides with azene and coumarin moieties as carbonic anhydrase inhibitors*, Arab. J. Chem. 16 (2023), pp. 104956. doi:10.1016/j.arabjc.2023.104956.

[20] J. Yang, D.L. Chen, P.C. Wang, B. Yang, and C.Z. Gao, *NIR phosphorescent cyclometalated platinum (II) complexes with CAIX targeted and nuclear penetration as potent anticancer theragnostic agents*, Eur. J. Med. Chem. 243 (2022), pp. 114702. doi:10.1016/j.ejmech.2022.114702.

[21] A. Elkamhawy, J. Woo, H. Nada, A. Angeli, T.M. Bedair, C.T. Supuran, and K. Lee, *Identification of novel and potent indole-based benzenesulfonamides as selective human carbonic anhydrase ii inhibitors: Design, synthesis, in vitro, and in silico studies*, Int. J. Mol. Sci. 23 (2022), pp. 2540. doi:10.3390/ijms23052540.

[22] H.T. Abdel-Mohsen, M.A. Omar, A. Petreni, and C.T. Supuran, *Novel benzenesulfonamide-thiouracil conjugates with a flexible N-ethyl acetamide linker as selective CA IX and CA XII inhibitors*, Arch. Pharm. 356 (2023), pp. 2200434. doi:10.1002/ardp.202200434.

[23] H. Nada, A. Elkamhawy, M.H. Abdellattif, A. Angeli, C.H. Lee, C.T. Supuran, and K. Lee, *4-anilinoquinazoline-based benzenesulfonamides as nanomolar inhibitors of carbonic anhydrase isoforms I, II, IX, and XII: Design, synthesis, in-vitro, and in-silico biological studies*, J. Enzyme Inhib. Med. Chem. 37 (2022), pp. 994–1004. doi:10.1080/14756366.2022.2055553.

[24] S. Janowska, D. Khylyuk, A. Gornowicz, A. Bielawska, M. Janowski, R. Czarnomysy, K. Bielawski, and M. Wujec, *Synthesis and anticancer activity of 1, 3, 4-thiadiazoles with 3-methoxyphenyl substituent*, Molecules 27 (2022), pp. 6977. doi:10.3390/molecules27206977.

[25] S. Janowska, D. Khylyuk, A. Bielawska, A. Szymanowska, A. Gornowicz, K. Bielawski, J. Noworól, S. Mandziuk, and M. Wujec, *New 1,3,4-thiadiazole derivatives with anticancer activity*, Molecules (2022), pp. 1814. doi:10.3390/molecules27061814.

[26] S.A. Ibrahim, M.M. Salem, H.A. Abd Elsalam, and A.A. Noser, *Design, synthesis, in-silico and biological evaluation of novel 2-amino-1, 3, 4-thiadiazole based hydrides as B-cell lymphoma-2 inhibitors with potential anticancer effects*, J. Mol. Struct. 1268 (2022), pp. 133673. doi:10.1016/j.molstruc.2022.133673.

[27] M. Vilková, M. Hudáčová, N. Palušeková, R. Jendželovský, M. Almáši, T. Béres, P. Fedoročko, and M. Kožurková, *Acridine based n-acylhydrazone derivatives as potential anticancer agents: Synthesis, characterization and ctdna/hsa spectroscopic binding properties*, Molecules 27 (2022), pp. 2883. doi:10.3390/molecules27092883.

[28] Y. Demir, F.S. Tokalı, E. Kalay, C. Türkeş, P. Tokalı, O.N. Aslan, K. Şendil, and Ş. Beydemir, *Synthesis and characterization of novel acyl hydrazones derived from vanillin as potential aldose reductase inhibitors*, Mol. Divers. (2022), pp. 1–21. doi:10.1007/s11030-022-10526-1.

[29] S. Al Bitar and H. Gali-Muhtasib, *The role of the cyclin dependent kinase inhibitor p21cip1/waf1 in targeting cancer: Molecular mechanisms and novel therapeutics*, Cancers 11 (2019), pp. 1475. doi:10.3390/cancers11101475.

[30] A. Işık, U.A. Çevik, I. Çelik, H.E. Bostancı, A. Karayel, G. Gündoğdu, U. İnce, A. Koçak, Y. Özkay, and Z.A. Kaplancıklı, *Benzimidazole-hydrazone derivatives: Synthesis, in vitro anticancer, antimicrobial, antioxidant activities, in silico DFT and ADMET studies*, J. Mol. Struct. 1270 (2022), pp. 133946. doi:10.1016/j.molstruc.2022.133946.

[31] F. Sozmen, M. Kucukoflaz, M. Ergul, Z.D.S. Inan, Y. Bozkurt, and D. Taydas, *Synthesis of multifunctional organic nanoparticles combining photodynamic therapy and chemotherapeutic drug release*, Macromol. Res. 30 (2022), pp. 61–69. doi:10.1007/s13233-022-0021-0.

[32] N. Valkova, F. Lépine, L. Labrie, M. Dupont, and R. Beaudet, *Purification and characterization of prba, a new esterase from* Enterobacter cloacae *hydrolyzing the esters of 4-hydroxybenzoic acid (parabens)*, J. Biol. Chem. 278 (2003), pp. 12779–12785. doi:10.1074/jbc.M213281200.

[33] E. Henke and U. Bornscheuer, *Esterases from* Bacillus subtilis *and B. stearothermophilus share high sequence homology but differ substantially in their properties*, Appl. Microbiol. Biotechnol. 60 (2002), pp. 320–326. doi:10.1007/s00253-002-1126-1.

[34] B.E.O. Bedir, E. Terzi, and O.O. Guler, *Differential in vitro effects of oncogenic pathway inhibitors on carbonic anhydrase-IX, xanthine oxidase, and catalase in colorectal cancer*, Int. J. Med. Biochem. 6 (2023), pp. 36–41.

[35] E.F. Pettersen, T.D. Goddard, C.C. Huang, E.C. Meng, G.S. Couch, T.I. Croll, J.H. Morris, and T. E. Ferrin, *UCSF ChimeraX: Structure visualization for researchers, educators, and developers*, Protein Sci. 30 (2021), pp. 70–82. doi:10.1002/pro.3943.

[36] P.R. Yadav, S.H. Basha, and P.K. Pindi, *Role of Thr199 residue in human β-carbonic anhydrase-II pH-dependent activity elucidated by microsecond simulation analysis*, J. Biomol. Struct. Dyn. 40 (2022), pp. 5016–5025. doi:10.1080/07391102.2020.1865203.

[37] J. Leitans, A. Kazaks, A. Balode, J. Ivanova, R. Zalubovskis, C.T. Supuran, and K. Tars, *Efficient expression and crystallization system of cancer-associated carbonic anhydrase isoform IX*, J. Med. Chem. 58 (2015), pp. 9004–9009. doi:10.1021/acs.jmedchem.5b01343.

[38] A. Daina, O. Michielin, and V. Zoete, *SwissADME: A free web tool to evaluate pharmacokinetics, drug-likeness and medicinal chemistry friendliness of small molecules*, Sci. Rep. 7 (2017), pp. 42717. doi:10.1038/srep42717.

[39] B.Y. Peng, A.K. Singh, C.H. Chan, Y.H. Deng, P.Y. Li, C.W. Su, C.Y. Wu, and W.P. Deng, *AGA induces sub-G1 cell cycle arrest and apoptosis in human colon cancer cells through p53-independent/p53-dependent pathway*, BMC Cancer 23 (2023), pp. 1–13. doi:10.1186/s12885-022-10466-x.